Index Modulated OFDM with Intercarrier Interference Cancellation

Yuke Li[1,2], Meng Zhang[1,2], Xiang Cheng[1,2], Miaowen Wen[3], and Liu-Qing Yang[2,4]
[1]State Key Laboratory of Advanced Optical Communication Systems and Networks
School of EECS, Peking University, Beijing, 100871, China
[2]State Key Laboratory of Management and Control for Complex Systems,
Institute of Automation, Chinese Academy of Sciences, Beijing, 100190, China
[3]School of Electronic and Information Engineering,
South China University of Technology, Guangzhou, 510640, China
[4]Department of Electrical and Computer Engineering, Colorado State University, Fort Collins, CO 80523, USA
Email: liyuke14@mails.ucas.ac.cn, {mannyzhang, xiangcheng}@pku.edu.cn,
eemwwen@scut.edu.cn, liuqing.yang@ieee.org.

***Abstract*—Index modulated orthogonal frequency division multiplexing (IM-OFDM) is a newly proposed technique, which achieves significantly improved error performance and peak-to-average power ratio (PAPR) in comparison with classical OFDM due to the activation of partial subcarriers. However, in the presence of inter-carrier interference (ICI), error detection of the subcarrier indices may easily occur, such that the performance of IM-OFDM is severely degraded and can be even worse than classical OFDM. To solve this problem, in this paper, we propose to tailor the ideas of classical ICI self-cancellation and two-path cancellation to IM-OFDM with two mapping methods, i.e., symmetric mapping and mirror mapping. Thanks to the joint design of the grouping and mapping methods, the proposed schemes inherit the IM-OFDM virtue of partially activated subcarriers but with reduced ICI. Monte Carlo Simulations validate that the proposed schemes significantly outperform conventional OFDM with ICI cancellation in additive white Gaussian noise (AWGN) channels with frequency deviation without sacrifice of the spectral efficiency and increase of the computational complexity.**

I. Introduction

OFDM is considered as a promising multicarrier transmission technique for high data rate wireless communication systems due to its sufficient robustness to handle radio channel impairments and high spectrum efficiency [1]. Recently, a novel OFDM scheme called IM-OFDM has been put forward [2] [3], which conveys the information bits not only by the M-ary constellation signals as in classical OFDM, but also by the indices of the active subcarriers. It has been verified that IM-OFDM achieves better error performance than conventional OFDM under perfect channel conditions [3]. IM-OFDM is also shown to have reduced PAPR [4], which significantly moderates the requirement of the amplifier dynamic range and therefore attributes the practicality of low-cost and highly energy efficient to the implementation of IM-OFDM. Thus, a number of studies emerge to further improve the performance of IM-OFDM. [5] proposes to group subcarriers in an interleaved manner and harvests significant performance improvement [6]. In [7], the authors discuss the optimal selection of the active subcarrier sets. [8], [9] apply index modulation to in-phase and quadrature components to improve the spectrum efficiency. The author in [10] proposes coordinate interleaving to achieve diversity gain in IM-OFDM.

Due to the fact that all subcarriers are strictly designed to be orthogonal, OFDM is vulnerable to frequency offset caused by Doppler shift and/or transceiver imperfection, which destroys the orthogonality among subcarriers and thus severely deteriorates the system performance. Unfortunately, ICI does much greater harm to IM-OFDM because the power leakage from the active subcarriers to the inactive ones significantly increases the probability of erroneous detection of subcarrier states and in turn misleads the detection of transmitted symbols at the active subcarriers. Thus, IM-OFDM demonstrates even worse performance than classical OFDM in the presence of ICI [11].

In the literature, numerous countermeasures have been proposed for OFDM system to combat ICI. Among them, ICI self-cancellation schemes [12]- [14] and two-path cancellation schemes [15]- [16] are widely accepted due to their simplicity and effectiveness. The main idea of ICI self-cancellation is to repeat the constellation symbols at the subcarriers according to specific mapping methods in a single OFDM block, so that the interference introduced by a specific subcarrier can be cancelled by its counterpart. Accordingly, in two-path cancellation schemes, the symbol repetitions are assigned to the adjacent OFDM blocks and ICI cancellation is done by the arithmetical operations between the two blocks. However, due to the special architecture of IM-OFDM, i.e., the partially activated subcarriers and subcarrier grouping, the mapping rules in traditional ICI cancellation schemes no longer hold. To benefit from the low PAPR of IM-OFDM under ICI, the joint design of IM-OFDM with ICI cancellation methods becomes an urgent and challenging task. Our previous work [17] proposes ICI self-cancellation with adjacent mapping for IM-OFDM in consideration of its easy implementation and effectiveness. However, we would like to address that adjacent mapping is suboptimal because the neighboring subcarriers in

978-1-4799-6664-6/16/$31.00 ©2016 IEEE

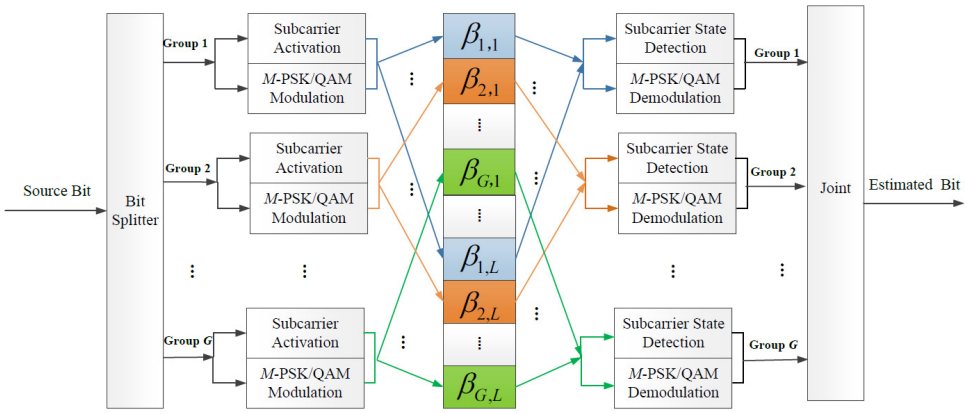

Fig. 1. Transceiver Structure of IM-OFDM.

each group are more likely to experience correlated fading, which is very common in vehicle-to-vehicle communications [18] [19] and will seriously degrade the system performance.

Motivated by this, in this paper, we leverage upon our earlier work and propose to introduce the symmetric mapping and mirror mapping methods to IM-OFDM systems to further improve the performance, which are more difficult to combine with IM-OFDM yet more effective. Specifically, we consider the principle of both classical ICI self-cancellation and two-path transmission schemes, and name them IM-OFDM with ICI self-cancellation and IM-OFDM with two-path cancellation, respectively. To design the schemes without sacrificing the nature of IM-OFDM, the mapping methods are jointly designed with the grouping and modulation methods, which are: 1) Symmetric Symbol Repetition (SSR), Symmetric Conjugate Symbol Repetition (SCSR), Mirror Symbol Repetition (MSR) and Mirror Conjugate Symbol Repetition (MCSR) for IM-OFDM with ICI self-cancellation, and 2) Symmetric Conversion Transmission (SCVT), Symmetric Conjugate Transmission (SCJT), Mirror Conversion Transmission (MCVT) and Mirror Conjugate Transmission (MCJT) for IM-OFDM with two-path cancellation. The transceiver structures of all the proposed schemes have similar overall complexity to that of conventional OFDM with ICI cancellation. It is shown via simulations that the proposed IM-OFDM with ICI cancellation schemes exhibit better system performance than traditional OFDM with ICI cancellation in AWGN channels under carrier frequency offset (CFO).

II. Overview of IM-OFDM

Fig. 1 shows the transceiver structure of the IM-OFDM. Assuming that there are in total N OFDM subcarriers, to ease the implementation of IM-OFDM, the total N subcarriers are split into G subblocks, each consisting of $L = N/G$ subcarriers. Then, the subcarrier activation and symbol modulation are performed within each subblocks according to the following procedure independently. Firstly, b out of L subcarriers in each subblock are set to be active. Then, b symbols are drawn from the M-ary PSK/QAM constellation to be sent from the active subcarriers, where M is the cardinality of the constellation. Finally, the remaining $(L-b)$ are zero-padded. Given L and b, there are in all $\mathbb{C}(L,b)$ combinations of active subcarrier indices, where $\mathbb{C}(\cdot,\cdot)$ denotes the binomial coefficient. Hence, $\lfloor \log_2 \mathbb{C}(L,b) \rfloor$ bits can be modulated to the active subcarrier indices via either a look-up table or the combinatorial method proposed in [3], with $\lfloor \cdot \rfloor$ being the floor operation. Therefore, in conjunction with the information bits carried by the b constellation symbols, IM-OFDM can convey a total of $\lfloor \log_2 \mathbb{C}(L,b) \rfloor + b \log_2 M$ bits per subblock. By concatenating the subcarrier subblocks, we obtain the original IM-OFDM block proposed in [3], which is grouped in a localized manner with its i-th element represented as $S_i, (i = 0, \cdots, N-1)$. To benefit from the uncorrelated channels and improve the system performance, the subcarriers are then go through an interleaver which results in $\Phi^g = \{g-1, g-1+G, \cdots, g-1+(L-1)G\}$ as depicted in Fig. 1, where $\Phi^g = \{\beta_{g,1}, \cdots, \beta_{g,L}\}$, $(g = 1, \cdots, G)$ represents the subcarrier indices of the g-th subblock, and $\Phi^1 \cup \cdots \cup \Phi^G = \{0, \cdots, N-1\}$. Clearly, the i-th element in localized grouping is placed to the j-th subcarrier after interleaving, with $j = \mathcal{I}(i) = i\%L \times G + \lfloor i/L \rfloor, (i = 0, \cdots, N-1)$. Next, the inverse fast Fourier transform (FFT) is applied and a cyclic prefix (CP) is added to the beginning of the time-domain OFDM symbol before sent from the transmit antenna.

At the receiver, after CP reduction, FFT and de-interleaving, the received signal within the g-th subblock in the frequency domain can be expressed by

$$Y_{\beta_{g,l}} = H_{\beta_{g,l}} X_{\beta_{g,l}} + W_{\beta_{g,l}}$$

where $X_{\beta_{g,l}}$ is the transmitted M-PSK/QAM symbol carried on the active subcarrier after interleaving, $H_{\beta_{g,l}}$ is the channel coefficient, and $W_{\beta_{g,l}}$ is the AWGN of variance N_0, at the $\beta_{g,l}$-th subcarrier, respectively. It is worth noting that the average transmit power of $X_{\beta_{g,l}}$ is P/b rather than P/L as in conventional OFDM with P being the total transmit power per subblock due to the presence of inactive subcarriers. Also, please keep in mind the difference and relationship between S_i and X_i, which plays an important role in understanding our proposed ICI cancellation schemes.

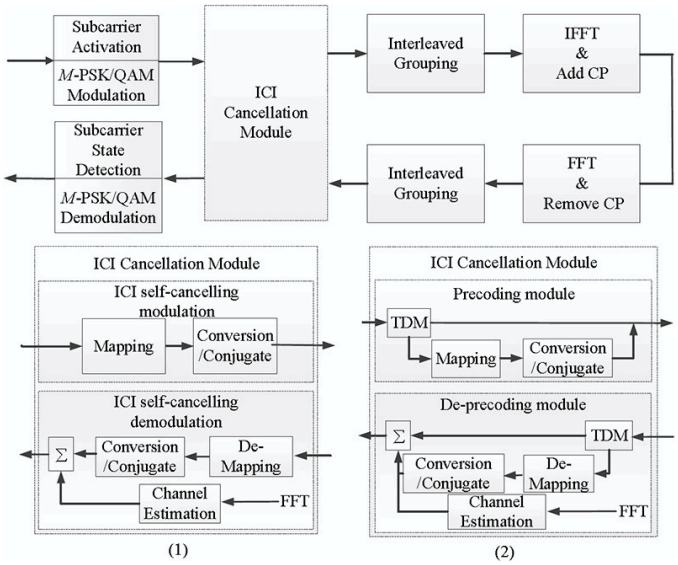

Fig. 2. Block diagram of a IM-OFDM transceiver with (1) ICI self-cancellation module and (2) two-path cancellation module.

To demodulate the information bits at the receiver, the log-likelihood ratio (LLR) detector of IM-OFDM evaluates the ratio of the posteriori probability of non-zero to that of zero for every subcarrier. This ratio gives information about the status of the corresponding subcarriers and can be written as

$$\lambda_{\beta_{g,l}} = \ln(b) - \ln(L-b) + \frac{|Y_{\beta_{g,l}}|^2}{N_0} + \ln\left(\sum_{\theta=1}^{M} \exp\left(-\frac{1}{N_0}|Y_{\beta_{g,l}} - H_{\beta_{g,l}} s_\theta|^2\right)\right), \quad (1)$$

where $\{s_1, \cdots, s_M\}$ represents the M-ary constellation symbols. The b subcarriers within the g-th subblock having maximum LLR values are determined to be active. Then the received signals associated with the determined active subcarriers are demodulated to get the estimated information bits. We note that the LLR detector may result in catastrophic error when deciding on an unused index combination. However, since the unused combinations are much less than the used ones, the performance penalty is negligible.

III. Proposed ICI Cancellation schemes

Since only partial subcarriers are set to be active, IM-OFDM is expected to have the potential of ICI suppression. However, this potential vanishes in real scenarios with ICI, because the interference between subcarriers severely disturbs the detection of active subcarrier indices, which leads to even worse performance than conventional OFDM. To solve the aforementioned problem, we tailor the classical ICI cancellation techniques of ICI self-cancellation and two-path cancellation to IM-OFDM and propose various jointly designed mapping strategies.

A. IM-OFDM with ICI self-cancellation

The block diagram of IM-OFDM with ICI self-cancellation is depicted in Fig. 2 (1), which can be described as follows. At the transmitter side, the data symbols and their counterparts are modulated on subcarrier pairs which are decided by different mapping methods so that the interference introduced by the subcarrier pairs can be self-cancelled. Then, at the receiver, the received signals on the subcarrier pairs are linearly combined to further reduce the residual ICI. As mentioned above, since adjacent subcarriers are more likely to experience correlated fading, we propose the joint design of interleaved grouping with symmetric mapping and mirror mapping in order to improve the frequency separation between the symbols.

In both schemes, before interleaved grouping, the first $N/2$ elements $\{S_0, \cdots, S_{N/2-1}\}$ already carry all the information to be transmitted, while the other half are padded with the repetition according to the mapping strategies. In this paper we consider two mapping strategies for IM-OFDM with ICI self-cancellation, namely symmetric mapping and mirror mapping, and design the index modulation criterion for them respectively.

1) Symmetric mapping: For symmetric mapping, the mapping rule is given by

$$\widetilde{S}_k = \begin{cases} S_k & k = 0, 1, \cdots, N/2-1 \\ \mathcal{O}\left(S_{N-1-k}\right) & k = N/2, \cdots, N-1 \end{cases},$$

where $\{S_k\}_{k=0}^{N/2-1}$ are simply modulated according to the criterion of the $N/2$ point and $G/2$ group IM-OFDM modulation, each group containing L elements, and $\{\widetilde{S}_k\}_{k=0}^{N-1}$ are the actual transmitted data symbols in the block before interleaving. $\mathcal{O}(\cdot)$ is the operation done to the counterpart of the symbol. Taking note that $\widetilde{S}_{N-1-k} = \mathcal{O}(\widetilde{S}_k), k = 0, 1, \cdots, N/2-1$, the elements are repeated in a symmetric manner, thus, it is termed symmetric-mapping. The conversion operation $\mathcal{O}(x) = -x$ and the conjugate operation $\mathcal{O}(x) = x^*$ are considered for IM-OFDM with ICI self-cancellation in this paper, which are named IM-OFDM with SSR and SCSR schemes, respectively. The obtained block then goes through an N point G group interleaver to obtain the interleaved OFDM blocks and is later sent from the transmitter.

At the receiver, after CP removal and FFT, the detected $\widetilde{S}_m$ can be obtained using the redundancy according to

$$\widehat{S}_m = \frac{H^*_{\mathcal{I}(m)} Y_{\mathcal{I}(m)} + \mathcal{O}(H^*_{\mathcal{I}(N-1-m)} Y_{\mathcal{I}(N-1-m)})}{|H_{\mathcal{I}(m)}|^2 + |H_{\mathcal{I}(N-1-m)}|^2}, \quad (2)$$

which is essentially maximum ratio combining (MRC).

2) Mirror mapping: In the proposed mirror mapping scheme, firstly, the 0-th element S_0 before interleaving is set to be zero, and index modulation is done within the rest $L-1$ elements in the first subblock. Then, the rest $G/2-1$ groups are modulated according to IM-OFDM to obtain $\{\widetilde{S}_k\}_{k=0}^{N/2-1}$. By setting $\widetilde{S}_{N/2} = 0$ and symmetrically map the left hand side elements to right hand side with respect to $\widetilde{S}_{N/2}$ regardless of $\widetilde{S}_0$, finally, we obtain

$$\widetilde{S}_k = \begin{cases} 0 & k = 0, N/2 \\ S_k & k = 1, 2, \cdots, N/2-1 \\ \mathcal{O}\left(S_{N-k}\right) & k = N/2+1, \cdots, N-1 \end{cases}.$$

Similar to symmetric mapping, with conversion and conjugate relationships adopted to the data copies, we have the IM-OFDM with MSR and MCSR schemes, respectively. The MRC equation of mirror mapping method is given by

$$\widehat{S}_m = \frac{H^*_{\mathcal{I}(m)} Y_{\mathcal{I}(m)} + \mathcal{O}(H^*_{\mathcal{I}(N-m)} Y_{\mathcal{I}(N-m)})}{|H_{\mathcal{I}(m)}|^2 + |H_{\mathcal{I}(N-m)}|^2}. \quad (3)$$

B. IM-OFDM with two-path cancellation

Fig. 2(2) depicts the system architecture of the ICI two-path cancellation schemes, which are integrated inside the precoding and decoding modules. Unlike ICI self-cancellation schemes, two-path cancellation schemes transmit the data copies in two concatenated IM-OFDM blocks, which are usually referred to as two independent paths separated by time division multiplexing (TDM). The two-path cancellation adopted symmetric mapping and mirror mapping methods designed for IM-OFDM are proposed in this subsection.

In general, for IM-OFDM with two-path cancellation, since the ICI cancellation is done with two OFDM symbols, we are able to simply set the first one to be the conventional IM-OFDM to ease the design. That is, one interleaved IM-OFDM symbol input $\{X_k\}_{k=0}^{N-1}$ will become two outputs $\{\overline{X}_k^{(1)}\}_{k=0}^{N-1}$ and $\{\overline{X}_k^{(2)}\}_{k=0}^{N-1}$ to be transmitted in adjacent time intervals, where the first OFDM symbol $\{\overline{X}_k^{(1)}\}_{k=0}^{N-1}$ is identical to the input OFDM symbol, i.e., $\overline{X}_k^{(1)} = X_k$ and the second OFDM symbol $\{\overline{X}_k^{(2)}\}_{k=0}^{N-1}$ is derived according to the subcarrier mapping rule illustrated in what follows.

1) Symmetric mapping: For symmetric mapping, the second OFDM symbol can be obtained as $\overline{X}_k^{(2)} = \mathcal{O}(X_{N-1-k})$, where $k = 0, 1, \cdots, N-1$. For ease of expression, if the conversion operation $\mathcal{O}(x) = -x$ is utilized for the symmetric operation, we refer to it as the IM-OFDM with SCVT scheme, if the conjugate operation is used, i.e., $\mathcal{O}(x) = x^*$, we call it the IM-OFDM with SCJT scheme.

Assuming that the channel remains invariant during the transmission of the two symbols, the MRC expression of the m-th symbol of the deinterleaved OFDM symbol at the receiver can be represented as

$$\widehat{S}_m = \frac{H^*_{\mathcal{I}(m)} \overline{Y}^{(1)}_{\mathcal{I}(m)} + \mathcal{O}\left\{H^*_{\mathcal{I}(N-1-m)} \overline{Y}^{(2)}_{\mathcal{I}(N-1-m)}\right\}}{|H_{\mathcal{I}(m)}|^2 + |H_{\mathcal{I}(N-1-m)}|^2}, \quad (4)$$

where $\overline{Y}_m^{(i)}$ is the m-th received signals corresponding to the i-th transmitted OFDM symbol ($i \in \{1, 2\}$).

2) Mirror mapping: Similarly, for mirror mapping, the second OFDM symbol obeys the mirror mapping rule as $\overline{X}_k^{(2)} = \mathcal{O}(X_{N-k})$. With either converse operation $\mathcal{O} = -x$ and conjugate operation $\mathcal{O} = x^*$, we have the IM-OFDM with MCVT scheme and IM-OFDM with MCJT scheme, respectively.

Again, the MRC expression of the m-th symbol of the interleaved OFDM block at the receiver can be represented as

$$\widehat{S}_m = \frac{H^*_{\mathcal{I}(m)} \overline{Y}^{(1)}_{\mathcal{I}(m)} + \mathcal{O}\left\{H^*_{\mathcal{I}(N-m)} \overline{Y}^{(2)}_{\mathcal{I}(N-m)}\right\}}{|H_{\mathcal{I}(m)}|^2 + |H_{\mathcal{I}(N-m)}|^2}. \quad (5)$$

C. LLR detector

For all proposed ICI cancellation schemes, LLR detector can be used to detect the states of subcarriers in each subblock by examining the LLR value

$$\begin{aligned}\lambda_m =& \ln(b) - \ln(L-b) + \frac{\Psi|\widehat{S}_m|^2}{N_0} \\ &+ \ln\left(\sum_{\theta=1}^{M} \exp\left(-\frac{\Psi}{N_0}|\widehat{S}_m - s_\theta|^2\right)\right),\end{aligned} \quad (6)$$

where $m \in \{L(g-1), L(g-1)+1, \cdots, Lg-1\}$, $g = 1, 2, \cdots, G$. Note that the MRC in (2)-(5) amplifies the noise power so the noise power in (6) should multiply by a factor of Ψ, where $\Psi = 1/\left(|H_{\mathcal{I}(m)}|^2 + |H_{\mathcal{I}(N-1-m)}|^2\right)$ for symmetric mapping and $\Psi = 1/\left(|H_{\mathcal{I}(m)}|^2 + |H_{\mathcal{I}(N-m)}|^2\right)$ for mirror mapping, respectively. Then b subcarriers within the g-th subblock having maximum LLR values are determined to be active. Particularly, in IM-OFDM with MSR, since the first subcarriers within 1-th subblock and $(G/2+1)$-th subblock are vacant, the LLR detector for these two aforementioned subblock can be obtained by replacing $\ln(L-b)$ with $\ln(L-1-b)$ in (6).

It can be readily shown that the computation complexity of MRC is $\boldsymbol{O}(N)$ and that of the LLR detector is $\boldsymbol{O}(LM)$, thus the computation complexity of our receiver is $\boldsymbol{O}(N + LM)$, which is comparable to that of conventional OFDM detector.

Due to the fact that the data repetitions are adopted by ICI self-cancellation and two-path cancellation techniques, the spectral efficiency of the proposed schemes is consequently half of IM-OFDM, given by $[\log_2 \mathbb{C}(L, b) + b \log_2 M]/2L$. With specific parameter selection, i.e., the length of the subblock L, the number of active subcarrier b and modulation order M, the spectral efficiency of the proposed schemes can be improved to exceed that of conventional OFDM with ICI cancellation schemes, given by $\log_2 M$.

IV. Simulation Results and Analysis

This section presents BER simulation results for the proposed schemes under CFO=0.05 over AWGN channels. The channel estimation is performed by the preamble, which is located prior to each OFDM data symbol and comprises an entire OFDM symbol known by both the transmitter and the receiver.

In the simulations, the total number of subcarriers is set to be $N = 64$. The following six types of OFDM schemes are considered for performance comparisons:

- OFDM with BPSK modulation;
- IM-OFDM with parameters chosen as: $G = 16$, $L = 4$, $b = 2$, and BPSK modulation.
- OFDM with ASR(ACSR) [11], SSR(SCSR) and MSR(MCSR) and QPSK modulation;
- OFDM with SCVT and MCVT and QPSK modulation;

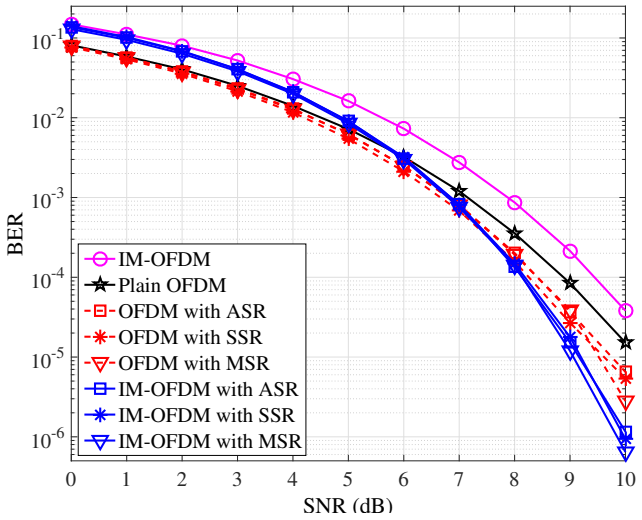

Fig. 3. Comparison results between OFDM with A(S,M)SR and IM-OFDM with A(S,M)SR.

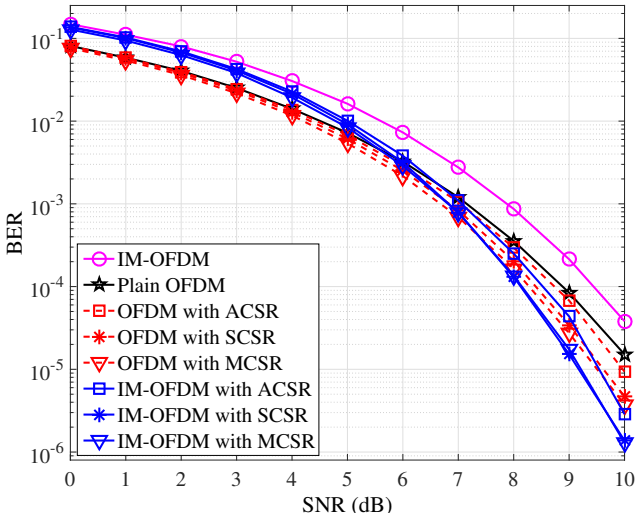

Fig. 4. Comparison results between OFDM with A(S,M)CSR and IM-OFDM with A(S,M)CSR.

- IM-OFDM with ASR(ACSR), SSR(SCSR) and MSR(MCSR) with parameters chosen as: $G = 16, L = 4, b = 3$, and QPSK modulation.
- IM-OFDM with SCVT and MCVT with parameters chosen as: $G = 16$, $L = 4$, $b = 3$, and QPSK modulation.

It can be readily found out that the above six schemes share the same spectral efficiency, i.e., 1 bps/Hz. Therefore, the comparison is fair in this sense. We measure BERs achieved by the aforementioned six schemes versus signal-to-noise ratio (SNR), which is defined as $\gamma = P/(NN_0)$, and obtain the following results.

Fig. 3 shows the comparison results between OFDM with A(S,M)SR and IM-OFDM with A(S,M)SR. As a reference, the Plain OFDM and IM-OFDM are also shown. As can be seen, the IM-OFDM performs worse than other schemes. This can be understood since with the existence of CFO, the inactive subcarrier is affected by the power leakage, and the subcarrier states become difficult to distinguish, which seriously deteriorates the system performance and makes it even worse than plain OFDM. Therefore, it is not surprising to observe a similar phenomenon in Figs. 4 and 5. On the other hand, we see from Fig. 3 that OFDM with A(S,M)SR perform better than plain OFDM, which validates the effectiveness of the ICI self-cancellation techniques in ICI reduction. As can be seen, in the low-to-moderate SNR region, IM-OFDM with A(S,M)SR perform worse than OFDM with A(S,M)SR. It can be explained by that when the SNR is low, the noise severely influence the detection of the active subcarriers. As SNR grows, the subcarrier state detection of the proposed schemes becomes accurate and the effect of ICI reduction appears. As can be seen, IM-OFDM with A(S,M)SR show better performance than other schemes when BER falls below 10^{-3}. This happens for two reasons. Firstly, the ICI generated from subcarrier pairs is suppressed with the help of ICI self-cancellation technique. In addition, thanks to index modulation, the number of active subcarriers which actually incur ICI is reduced to $(b/L)N$. From Fig. 3, we can see that the performance of IM-OFDM with SSR is comparable to IM-OFDM with ASR over AWGN channel. IM-OFDM with MSR outperforms both of them slightly because there are two extra subcarriers are set to be vacant in MSR, thus the number of subcarriers which incur ICI is further reduced.

In Fig. 4, the comparison results between OFDM with A(S,M)CSR and IM-OFDM with A(S,M)CSR is shown. With conjugation operation, IM-OFDM with A(S,M)CSR performs superior to other schemes in middle-to-high SNR region. However, the curve of IM-OFDM with ACSR raised a little because the self-interference (SI) is introduced due to the nature of adjacent conjugate symbols [13]. Even so, the performance of IM-OFDM with ACSR still outperforms the corresponding OFDM with ACSR.

Fig. 5 shows the comparison results between OFDM with S(M)CVT and IM-OFDM with S(M)CVT. As shown in the figure, OFDM with S(M)CVT and IM-OFDM with S(M)CVT outperform IM-OFDM and plain OFDM. As can be seen, when BER falls below 10^{-3}, IM-OFDM with S(M)CVT shows better BER performance than other scheme. It can be observed that the performance of IM-OFDM with SCVT is close to that of IM-OFDM with MCVT, this is due to the fact that MCVT has the same average carrier-to-interference power ratio (CIR) performance as the SCVT when only CFO exists. However, when IQ imbalance occurs, MCVT may performs superior to SCVT [14].

Fig. 6 shows the comparison results between IM-OFDM with A(S,M)SR and IM-OFDM with S(M)CVT. It can be seen that IM-OFDM with ICI self-cancellation scheme slightly outperform IM-OFDM with two-path cancellation schemes. This happens because only half of all subcarriers in ICI self-cancellation induce ICI among each other, while all subcarriers in two-path schemes are the source of interference. However,

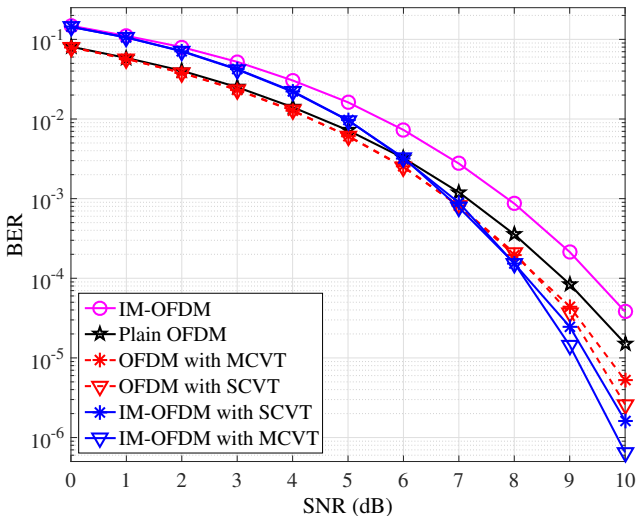

Fig. 5. Comparison results between OFDM with S(M)CVT and IM-OFDM with S(M)CVT.

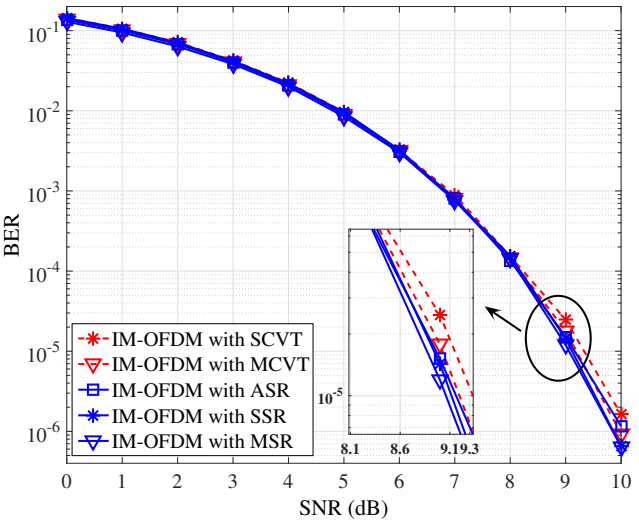

Fig. 6. Comparison results IM-OFDM with A(S,M)SR and IM-OFDM with S(M)CVT.

the difference between IM-OFDM with A(S,M)SR and IM-OFDM with S(M)CVT is small.

V. Conclusions

In this paper, ICI self-cancellation and two-path cancellation have been specially tailored to IM-OFDM systems with different mapping methods (adjacent/symmetric/mirror) and operations (conversation/conjugation) adopted to the counterpart of the symbols. The combinations result in several ICI cancellation schemes of IM-OFDM with A(C)SR, S(C)SR, M(C)SR, SC(J)VT and MC(J)VT and all schemes preserve the IM-OFDM nature of partially activated subcarriers. The simulation results have shown that while mirror-mapping and ICI self-cancellation599949 provide the best performance in cooperation with IM-OFDM, all proposed IM-OFDM with ICI cancellation schemes outperform traditional OFDM with ICI cancellation in AWGN channels with CFO.

VI. Acknowledgement

This work was supported in part by the National Natural Science Foundation of China under Grants 61571020, 61501461, and 61501190, the National Science Foundation under Grant CNS-1343189, the National 863 Project under Grants 2014AA01A706, the Major Project from Beijing Municipal Science and Technology Commission under Grant D151100000115004, and the Early Career Development Award of SKLMCCS (Y3S9021F34).

References

[1] R. Nee and R. Prasad, *OFDM for Wireless Multimedia Communications*, Artech House Publishers, Mar. 2000.

[2] R. A.Alhiga and H. Haas, "Subcarrier-index modulation OFDM," in *Proc. IEEE 20th International Symposium on Personal, Indoor and Mobile Radio Communications*, Tokyo, Japan, 2009, pp. 177-181.

[3] E. Basar, U. Aygolu, E. Panayirci, and H. V. Poor, "Orthogonal frequency division multiplexing with index modulation," *IEEE Trans. Signal Process.*, vol. 61, no. 22, pp. 5536-5549, Nov. 2013.

[4] L. Xiao, B. Xu, H. Bai, Y. Xiao, X. Lei, S. Li, "Performance evaluation in PAPR and ICI for ISIM-OFDM systems," in *Proc. IEEE HMWC 2014*, Beijing, China, 2014, pp. 84-88.

[5] X. Cheng, M. Wen, L. Yang, and Y. Li, "Index Modulated OFDM with Interleaved Grouping for V2X Communications," in *Proc. IEEE ITSC 2014*, Qingdao, China, 2014, pp. 1097-1104.

[6] M. Wen, X. Cheng, M. Ma, B. Jiao, and H. V. Poor, "On the Achievable Rate of OFDM with Index Modulation, *IEEE Trans. on Signal Processing*, vol. 64, no. 8, pp. 1919-1932, Apr. 2016.

[7] M. Wen, X. Cheng, and L. Yang, "Optimizing the energy efficiency of OFDM with index modulation," in *IEEE Int. Conf. Commun. Systems*, Nov. 2014, pp. 31-35.

[8] R. Fan, Y. Yu, and Y. Guan, "Generalization of orthogonal frequency division multiplexing with index modulation," *IEEE Trans. Wireless Commun.*, vol. 14, no. 10, pp. 5350-5359, May 2015.

[9] B. Zheng, F. Chen, M. Wen, F. Ji, H. Yu, and Y. Liu, "Low-Complexity ML Detector and Performance Analysis for OFDM with In-Phase/Quadrature Index Modulation," *IEEE Commun. Lett.*, doi: 10.1109/LCOMM.2015.2474863.

[10] E. Basar, "OFDM with index modulation using coordinate interleaving," *IEEE Wireless Commun. Lett.*, vol. 4, no. 4, pp. 381-384, Apr. 2015.

[11] M. Wen, Y. Li, X. Cheng, and L. Yang, "Index modulated OFDM with ICI self-cancellation in underwater acoustic communications," in *Proc. IEEE Asilomar Conference on Signals, Systems, and Computers, Pacific Grove*, CA, USA, Nov. 2014, pp. 338-342.

[12] Y. Zhao, S-G. Haggman, "Intercarrier interference self-cancellation scheme for OFDM mobile communication systems," *IEEE Trans. Commun.*, vol. 49, no. 7, pp. 1185-1191, Jul. 2001.

[13] K. Sathananthan, C. R. N. Athandage, and B. Qin, "A Novel ICI Cancellation Scheme to Reduce both Frequency Offset and IQ Imbalance Effects in OFDM," in *Proc. IEEE 9th Int. Symp. Comput. Commun.*, vol.2, July 2004, pp. 708-713.

[14] M. Wen, X. Cheng, X. Wei, B. Ai, and B. Jiao, "A novel effective ICI self-cancellation method," in *Proc. IEEE Globecom*, Houston, TX, USA, Dec. 2011, pp. 1-5.

[15] M. Wen, X. Cheng, L. Yang, and B. Jiao, "Two-path transmission framework for ICI reduction in OFDM systems," in *Proc. IEEE Globecom*, Atlanta, GA, Dec. 2013, pp. 3716-3721.

[16] X. Cheng, Q. Yao, M. Wen, C.-X. Wang, L. Song, and B. Jiao, "Wideband channel modeling and ICI cancellation for vehicle-to-vehicle communication systems," *IEEE J. Sel. Areas in Commun.*, vol. 31, no. 9, pp. 434-448, Sept. 2013.

[17] M. Wen, X. Cheng, L. Yang, Y. Li, X. Cheng, and F. Ji, "Index Modulated OFDM for Underwater Acoustic Communications, *IEEE Commun. Mag.*, 2016 (accepted).

[18] C.-X. Wang, X. Cheng, and D. Laurenson, "Vehicle-to-vehicle channel modeling and measurements: recent advances and future challenges, *IEEE Commun. Mag.*, vol. 47, no. 11, pp. 96 C 103, Nov. 2009.

[19] X. Cheng, C.-X. Wang, B. Ai, and H. Aggoune, "Envelope Level Crossing Rate and Average Fade Duration of Non-Isotropic Vehicle-to-Vehicle Ricean Fading Channels, *IEEE Trans. Intell. Transp. Syst.*, vol. 15, no. 1, pp. 62-72, Feb. 2014.